

UNDERSTANDING SPACE WEATHER

Author(s): Keith Strong, Nicholeen Viall, Joan Schmelz and Julia Saba

Source: *Bulletin of the American Meteorological Society*, Vol. 98, No. 12, Disaster Dynamics: Communicating Risk in a New Information Age (December 2017), pp. 2593-2602

Published by: American Meteorological Society

Stable URL: <https://www.jstor.org/stable/10.2307/26639694>

---

JSTOR is a not-for-profit service that helps scholars, researchers, and students discover, use, and build upon a wide range of content in a trusted digital archive. We use information technology and tools to increase productivity and facilitate new forms of scholarship. For more information about JSTOR, please contact support@jstor.org.

Your use of the JSTOR archive indicates your acceptance of the Terms & Conditions of Use, available at <https://about.jstor.org/terms>



American Meteorological Society is collaborating with JSTOR to digitize, preserve and extend access to *Bulletin of the American Meteorological Society*

JSTOR

# UNDERSTANDING SPACE WEATHER

## Part III: The Sun's Domain

KEITH STRONG, NICHOLEEN VIALL, JOAN SCHMELZ, AND JULIA SABA

The solar wind is a continuous, varying outflow of high-temperature plasma, traveling at hundreds of kilometers per second and stretching to over 100 au from the Sun.

This paper is the third in a series of five papers about understanding the phenomena that cause space weather and their impacts. These papers are a primer for meteorological and climatological students who may be interested in the outside forces that directly or indirectly affect Earth's neutral atmosphere. The series is also designed to provide background information for the many media weather forecasters who often refer to solar-related phenomena such as flares, coronal mass ejections (CMEs), coronal holes, and geomagnetic storms. Often those presentations are misleading or definitively wrong.

Our intention is to provide a basic context so that they can produce more informative and interesting program content with respect to space weather.

Strong et al. (2012, hereafter Part I) described the production of solar energy and its tortuous journey from the solar core to the surface. That paper dealt with long-term variations of the solar output. Strong et al. (2017, hereafter Part II) addressed issues related to short-term solar variability (primarily flares and CMEs). This paper (Part III) deals with the variations in the outflow of particles from the Sun throughout the solar system to its outer boundaries: the Sun's domain (see Fig. 1). The forthcoming Part IV ("The Sun-Earth Connection") will deal with how the variable solar radiation, magnetic field, and particle outputs interact with Earth's magnetic field and atmosphere. The concluding Part V ("Impacts on Life and Society") will discuss the tangible effects of space weather on our increasingly technology-dependent civilization.

The quiescent state of the Sun produces the continual stream of particles and magnetic fields called the solar wind. The Sun undergoes frequent violent explosions resulting in solar flares and CMEs. Both are generally understood to be the result of a huge magnetic reconnection event on the Sun. A solar flare is the rapid increase in photons (radiation from  $\gamma$  rays to radio waves) and propagates isotropically to arrive at Earth about 8 min later (i.e., at the speed of light) to

**AFFILIATIONS:** STRONG,\* VIALL, AND SABA\*—NASA Goddard Space Flight Center, Greenbelt, Maryland; SCHMELZ—Universities Space Research Association, Columbia, Maryland, and University of Memphis, Memphis, Tennessee

\* Emeritus

**CORRESPONDING AUTHOR:** Dr. Keith T. Strong, drkts@aol.com

*The abstract for this article can be found in this issue, following the table of contents.*

DOI:10.1175/BAMS-D-16-0204.1

In final form 23 January 2017

©2017 American Meteorological Society

For information regarding reuse of this content and general copyright information, consult the [AMS Copyright Policy](#).

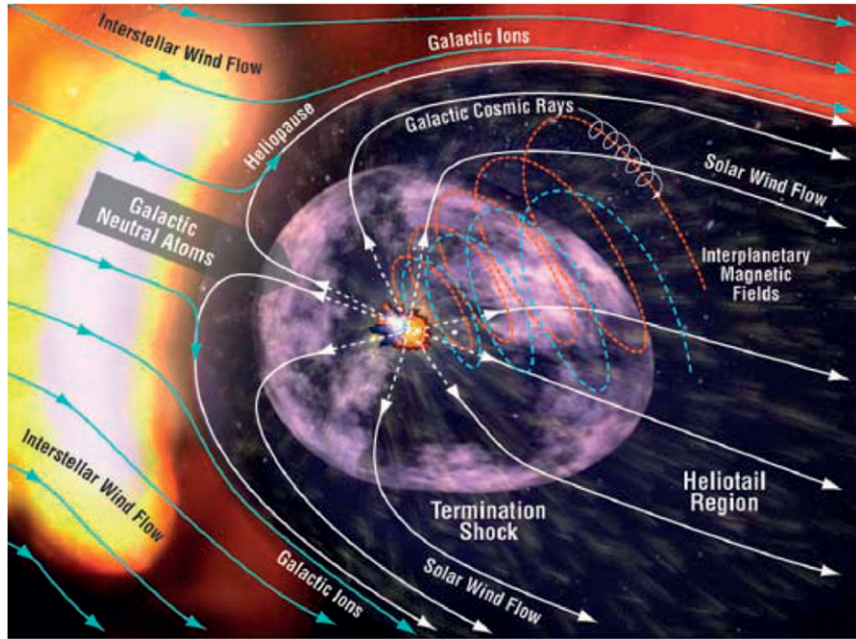


**FIG. 1.** The domain of the Sun (the heliosphere) stretches from the Sun itself (center of image) to the edge of interstellar space. The ambient conditions in the inner solar system are determined by the nature of the solar wind. The outer edge of the solar system comprises zones characterized by the solar wind's interaction with the interstellar medium as the solar system plows through it. These interactions give rise to many complex physical processes that can affect our space weather. [Figure from Gilbert et al. (2009).]

impact Earth's thermosphere and ionosphere. A CME consists of the magnetic field and plasma expelled from the Sun into interplanetary space at several hundred kilometers per second and so can arrive at Earth days later. CMEs often erupt at speeds significantly different from that of the ambient solar wind. Both the initial magnetic reconnection and the resulting CME shock can accelerate particles to extremely high energies, creating solar energetic particles (SEPs) [see the reviews by Schwenn (2006) and Pulkkinen (2007)]. There is a higher occurrence of these solar explosions during solar maximum, although solar flares and CMEs can occur during solar minimum too.

**CORONAL HOLES AND THE SOLAR WIND.** EUV and X-ray images of the solar corona show large areas of low emissions, called coronal holes. The solar magnetic fields in coronal holes are relatively weak, predominantly radial, and connected to interplanetary magnetic fields. As the primary emission process in the lower corona is collisional excitation, which increases rapidly with temperature and density, coronal holes, being less dense and cooler than their surroundings, emit less radiation and hence appear darker.

Where the coronal fields are open (i.e., one end of the field line connects directly back to

the solar surface while the other end is connected to the heliospheric fields), the solar wind particles can stream out into interplanetary space. The Sun exports nearly  $2 \text{ Mt s}^{-1}$  of solar wind particles, mostly protons and electrons with some  $\alpha$  particles (He nuclei) and trace amounts of heavier elements.

The solar wind is accelerated to speeds of  $200\text{--}800 \text{ km s}^{-1}$  with a mean of  $\sim 450 \text{ km s}^{-1}$  at Earth. These flows exceed both the speed of sound and Alfvén velocity (the speed at which a low-frequency oscillation of the ions and magnetic field propagates through the medium). Ultimately, the energy that heats the solar corona and accelerates the solar wind comes from the magnetic energy built up

by the tangling photospheric motions. However, the physical mechanisms by which the Sun accelerates the plasma to these high speeds are, as yet, unknown.

The electron density of the solar wind starts out at over  $10^8 \text{ cm}^{-3}$  near the Sun and falls with distance from the Sun according to the inverse square law, ranging from  $2$  to  $50 \text{ cm}^{-3}$  at  $1 \text{ au}$  (where  $1 \text{ au} \equiv 149\,597\,870\,700 \text{ m}$ ). The solar wind is charge neutral, so that the proton and electron number densities are essentially the same, with the protons carrying most of the momentum. The total mass of the solar wind impinging on the entire Earth is about  $7 \text{ kg s}^{-1}$ , carrying a kinetic energy on the order of  $7 \times 10^{11} \text{ J}$  (i.e., about 0.0004% of the radiant energy Earth receives from the Sun in a second). However, most of the solar wind is diverted around Earth by the magnetosphere except during solar storms, so the actual mass and energy flux directly injected into geospace from the solar wind is considerably less.

The solar wind is basically a collisionless plasma whose flow becomes faster than collisions can equilibrate the ionization states, so they become "frozen in" and do not evolve subsequently with propagation. Consequently, the concept of temperature is different in the solar wind from that in a collisional gas like Earth's atmosphere. The different components of the

solar wind are coupled via wave-particle interactions as opposed to classical Coulomb collisions. The solar wind velocity distribution often has a Maxwellian form; the protons have a thermal velocity of about  $40 \text{ km s}^{-1}$ , which corresponds to a temperature of about 0.1 MK.

The solar wind permeates the entire solar system, a huge volume of space (of order  $10^{31} \text{ km}^3$ ). It is currently sampled in situ by a small fleet of interplanetary spacecraft at just a few points, mostly in orbits near the ecliptic plane or around a few of the planets. Many of the solar wind phenomena vary on a wide range of temporal and spatial scales. Therefore, these intermittent measurements leave key properties of the solar wind (e.g., temperature, composition, velocity, density, ionization state, and magnetic field) vastly undersampled.

Remote sensing instruments give a global view of the solar wind and CMEs as they flow out from the Sun. For example, the simultaneous white-light images from the two Solar Terrestrial Relations Observatory (STEREO) spacecraft (Howard et al. 2008) allow for a 3D reconstruction of CMEs, from which the electron density and speed can be estimated. The images can also be used to measure relative density changes and the velocity of the ambient solar wind, particularly where the solar wind is first accelerated (e.g., Sheeley 1999; Viall et al. 2010).

Coronal holes exist almost continuously throughout the ~11-yr solar activity cycle. Solar wind from coronal holes flows outward at speeds up to  $800 \text{ km s}^{-1}$ , thus being termed the high-speed solar wind (McComas et al. 1998). When coronal holes appear at lower latitudes, especially when they cross the solar equator, these high-speed streams of particles sweep past Earth once every solar rotation (~27 days). Higher-latitude coronal holes can also become geoeffective as a result of the tilt of the solar magnetic dipole and the inclination of the solar spin axis with respect to the ecliptic. These recurring patterns can last for many months, making their impacts somewhat predictable (see Fig. 2).

In the corona the magnetic pressure exceeds the plasma pressure, so the magnetic field constrains and guides the high-temperature plasma. However, as the solar corona transitions into the solar wind, the ratio of the plasma pressure to the magnetic pressure changes, and the plasma pressure takes control. In the accelerated solar wind, that ratio is on average 1, but can range from ~0.1 to 10. In the region near the magnetic equator, the magnetic field pressure declines and the ratio can become very large.

Once accelerated, the solar wind plasma flows out radially, so the magnetic field, constrained by

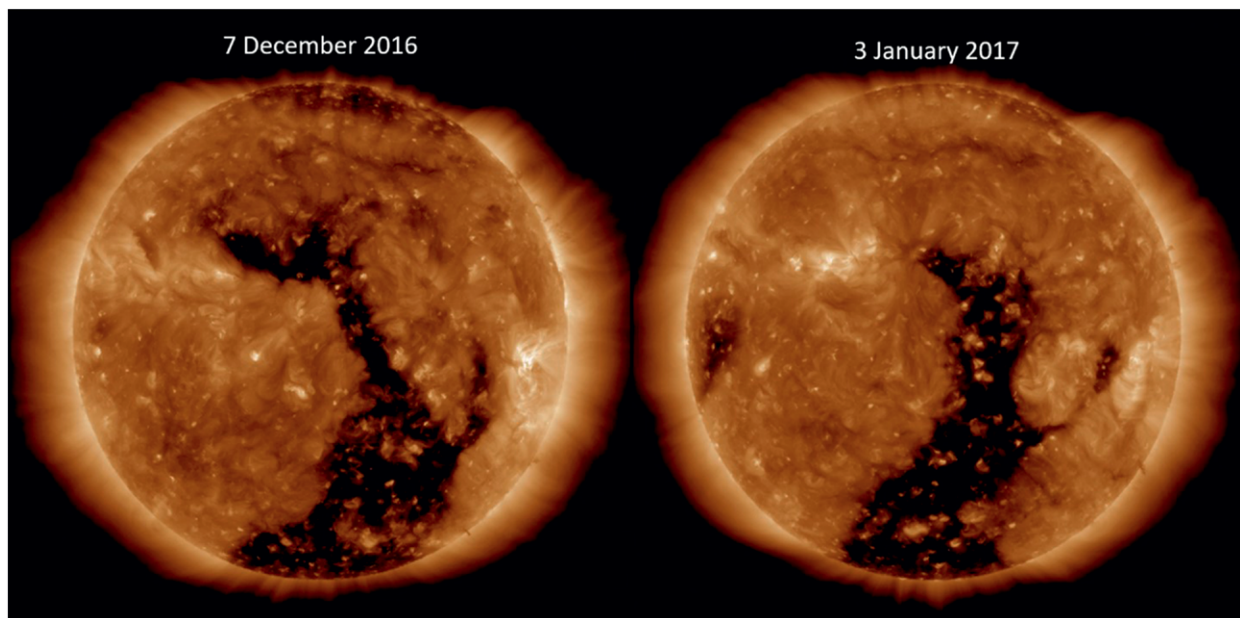


**FIG. 2.** The dark areas are coronal holes with radial magnetic fields connected to the interplanetary fields. They are cooler and less dense than the rest of the corona. The large transequatorial coronal hole at the disk's center is imaged on (left) 7 Dec 2016 and (right) again on 3 Jan 2017 (i.e., about one solar rotation later). This coronal hole formed during Nov 2016 (see Fig. 7 in Part II) and lasted a total of 9 months. Interestingly, coronal holes do not seem to share the same differential rotation rate as that of the photosphere. The northern polar coronal hole is also faintly visible (top). [The Fe XII image at 19.3 nm (about 1.2 MK) is courtesy of the National Aeronautics and Space Administration's (NASA) Solar Dynamics Observatory (SDO) Atmospheric Imaging Assembly (AIA).]

the plasma flow and anchored on the surface of the rotating Sun, forms a spiral. This winding up of the magnetic field amplifies its strength. The magnetic fields in the two hemispheres have opposite polarities and so form a volume with a very thin current layer, called the heliospheric current sheet (HCS). It has a complex three-dimensional structure primarily as a result of the tilt of the solar magnetic dipole axis relative to the Sun's rotational axis (see Fig. 3).

### THE FAST AND SLOW SOLAR WINDS.

The "slow" solar wind comes from regions associated with the equatorial streamer belt, which has predominantly closed field lines (McComas et al. 1998). Its origin remains controversial (Cranmer 2009). Some argue that it comes from open fields that reconnect with quiet-sun and/or active-region loops, releasing previously confined plasma (e.g., Fisk 2003), likely occurring at the boundary between open and closed field lines (Antiochos et al. 2011). Others argue that it comes from the boundaries of coronal holes where the field is exclusively open (e.g., Wang and Sheeley 1990). The slow solar wind moves at less than half the speed of the fast wind; it is much denser, has a lower temperature (as measured by its Maxwellian distribution), and is much more variable.

Though the separation of the fast and slow winds was based historically on velocity (e.g., Geiss et al. 1995), it is even more pronounced in elemental charge-state ratios, such as highly ionized oxygen and carbon, for example,  $O^{+7}/O^{+6}$  or  $C^{+6}/C^{+5}$  (Von Steiger et al. 2000). The separation is also apparent in the abundances of  $\alpha$  particles (Kasper et al. 2007)

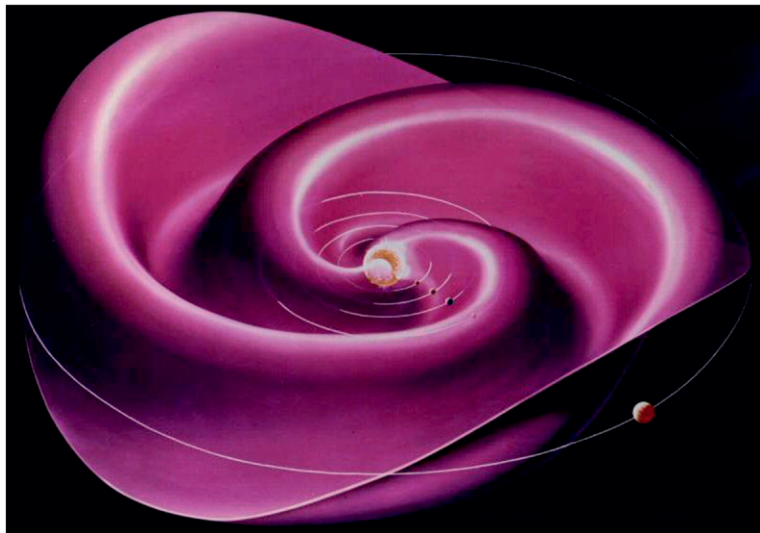


**FIG. 3. The solar rotation causes the HCS to take the form of a spiral. It is tilted with respect to the Sun's equator, forming this complicated 3D structure: the heliospheric "ballerina skirt" (Wilcox et al. 1980).**

and elements with differing first ionization potential (FIP; Geiss and Gloeckler 1998). This is because, unlike plasma properties such as density, velocity, or magnetic field that can evolve with acceleration and propagation from the Sun, elemental charge states and abundances are set in the lower solar atmosphere and do not evolve. Therefore, they can be used to track components of the solar wind, SEPs, and CMEs back to their source regions.

Elemental abundances are measured in the solar corona and photosphere through spectral analysis of data taken remotely, for example, from the Coronal Diagnostic Spectrometer on the Solar and Heliospheric Observatory (SOHO) at L1 (Harrison et al. 1995) and more recently from the Interface Region Imaging Spectrograph (De Pontieu et al. 2014). In contrast, the solar wind, SEPs, and CMEs are measured in situ by identifying and counting particles, therefore providing a more direct measurement of the plasma composition.

Regions of the corona with closed magnetic fields have different elemental abundances from their photospheric counterparts: they are enhanced in elements with low FIP ( $<10$  eV) relative to those with high FIP ( $>11$  eV). This fractionation most likely results from a separation of ions and neutrals in a layer of the solar atmosphere with a temperature of 6,000–10,000 K, where low-FIP elements are partially ionized and so can be more easily trapped within magnetic loops.

The fast wind has lower charge states and is not enhanced in low-FIP elements, having nearly photospheric abundances. This is consistent with the fast wind originating from cooler coronal holes, and the plasma streaming straight out without time for FIP fractionation. The slow wind has higher charge states and a larger, more variable fractionation (factor  $>2.5$ ), and is enhanced in low-FIP elements as in the corona. This is consistent with the slow wind originating from or near the hotter coronal loops, especially in the streamer belt.

The distribution of the low- and high-speed solar winds changes with the solar cycle (see results from Ulysses flybys in Fig. 4). Near solar minimum, the magnetic configuration of the corona is less complex, and low-speed wind tends to be concentrated near the equator, while the high-speed wind tends to be concentrated at the poles. However,

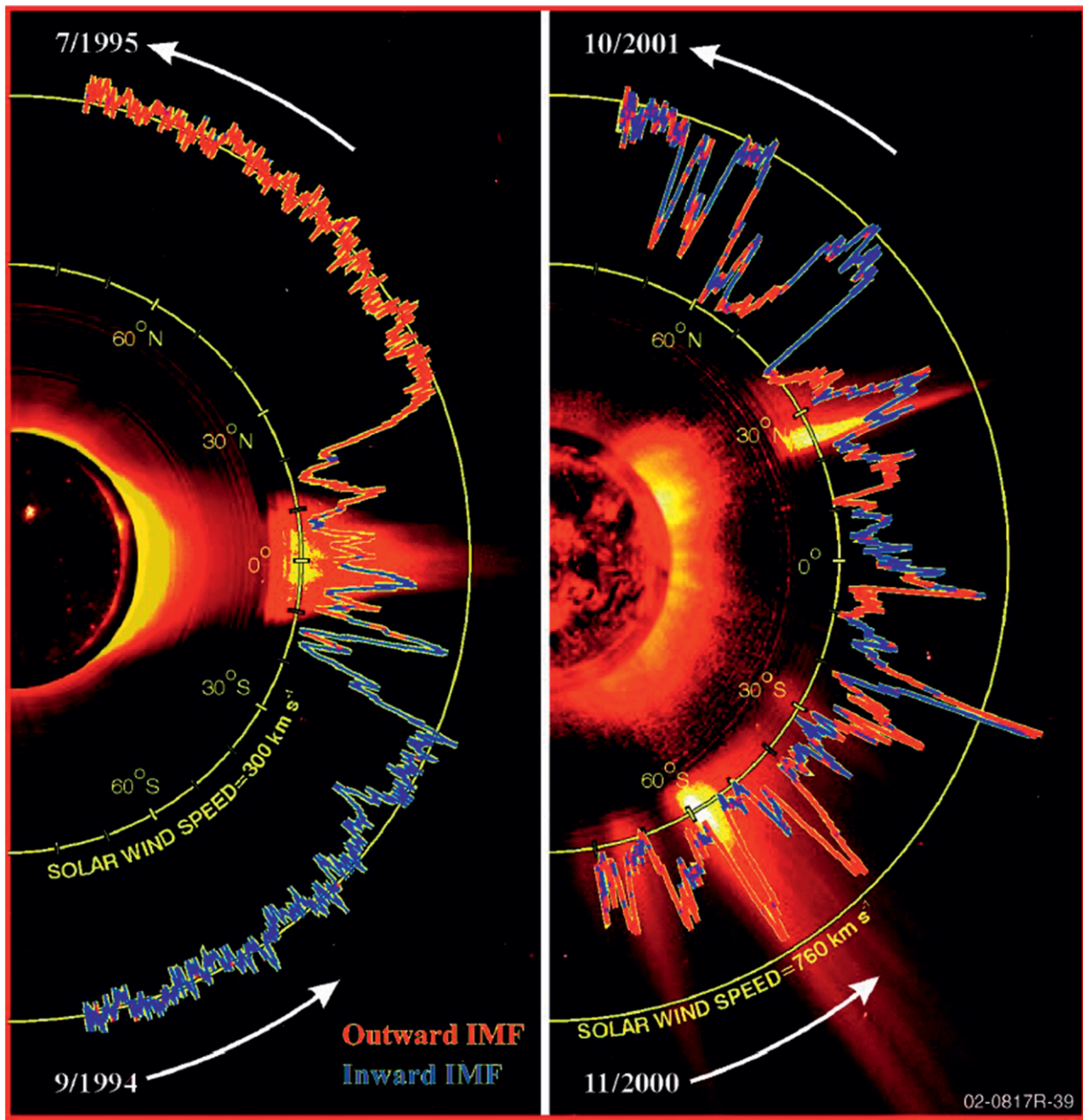


**FIG. 4.** The structure of the solar wind at solar minimum during (left) 1994/95, mostly high-speed streams at high latitudes with a narrow band of low-speed wind near the HCS, is contrasted with that at solar maximum during (right) 2000/01, where there is a mixture of high- and low-speed streams over most latitudes. (Source: NASA Ulysses; [http://solarprobe.gsfc.nasa.gov/solarprobe\\_science.htm](http://solarprobe.gsfc.nasa.gov/solarprobe_science.htm).)

as solar maximum approaches, the streamer belt and heliospheric current sheet become highly complex and the structure of the solar wind becomes very fragmented. Speed and density are anticorrelated in the solar wind, so for both the fast and slow winds, the mass flux is approximately constant. A clearly bimodal solar wind is no longer present at solar maximum, and at 1 au in the ecliptic, the velocity distribution becomes singly peaked and broad.

The acceleration of the solar wind is protracted; remote sensing measurements have found that the solar wind accelerates to over  $200 \text{ km s}^{-1}$  relatively low in the solar atmosphere but does not attain its final velocity until it has reached at least five solar radii (McComas et al. 2007). This has fundamental implications for the nature of the accelerator and implies that wave-particle interactions must play a role. While many believe that waves are the most

important accelerator, others argue that waves do not impart nearly enough energy.

Magnetic reconnection events may accelerate the wind, but, even then, waves resulting from the reconnection process likely play some role in the acceleration. In the classic, isothermal solar wind solution (Parker 1958), the corona is maintained at 1 MK and the acceleration occurs over large distances. Parker (1989) himself proposed that the mechanism that maintains the corona at about 1 MK is due to small magnetic reconnection events that he called nanoflares. The flow and acceleration profile is merely a reflection of the hot plasma responding to pressure gradients from the outer bounds of the heliosphere. In essence, the energy needed to maintain the corona at 1 MK is the energy that ultimately leads to its acceleration.

There are complex interactions between regions where the fast and slow solar winds are adjacent. These regions are referred to as corotating interaction regions (CIRs). A high-speed region trailing behind a low-speed region will catch up and overtake it. During this process the plasma on the leading edge of the high-speed stream will become compressed and a shock may form. Most shocks from CIRs do not form until beyond 1 au, but the steepening of the CIRs and discontinuities in plasma properties are important drivers of magnetospheric dynamics at different latitudes. Additionally, the steepened CIR shock beyond 1 au will be a concern for manned missions to Mars and beyond.

The slow solar wind that dominates the ecliptic is highly dynamic and variable on a variety of temporal and spatial scales, from those associated with solar rotation to those associated with kinetic physics. Some

of this variability is directly tied to differing coronal source regions, while some is nondeterministic and so is described through turbulence theory. Regardless of the source, these variations can be very important for energy transfer into Earth's magnetosphere. For example, density and/or velocity changes typical of the ambient solar wind will result in dynamic pressure changes and will compress and dilate the magnetosphere, driving waves and energizing particles.

Furthermore, although the magnetic field direction changes in a turbulent manner, whenever the  $z$  component of the magnetic field changes to point southward (a negative  $B_z$ ), there is magnetic reconnection on the dayside magnetosphere, leading to increased solar wind–magnetosphere coupling, even under ambient conditions. CMEs can have prolonged periods of negative  $B_z$  as a result of their twisted flux rope nature, resulting in extended periods of dayside magnetic reconnection; this is a way that they impart large energy changes into Earth's magnetosphere.

## SOLAR WIND INTERACTIONS WITH THE SOLAR SYSTEM.

The solar wind changes its nature, becoming more tenuous as it moves away from the Sun; it also encounters a range of objects with very different properties and interacts uniquely with each. The main properties of an object that determine how it reacts to the solar wind are the strength and orientation of its magnetic field and the nature of its atmosphere (see Table 1).

The rocky inner planets interact very differently with the solar wind compared to the gas giants. They also differ greatly from each other:

Mercury has only a trace atmosphere but possesses a weak dipolar magnetic field. The Mercury Surface,

**TABLE I. Comparison of planetary atmospheric and magnetic properties.**

	Intrinsic magnetic field	Surface atmospheric pressure	Magnetosphere	Ionosphere
Mercury	0.01	0	Yes	None
Venus	$10^{-5}$	90	Induced	Yes
Earth	1	1	Yes	Yes
Moon	0	0	No	No
Mars	0.02–0.06	0.06	Local	Yes
Jupiter	$2 \times 10^4$	N/A*	Yes	Yes
Saturn	600	N/A	Yes	Yes
Uranus	50**	N/A	Yes	Yes
Neptune	30**	N/A	Yes	Yes
Comets	0	Variable	Induced	Variable

\*The highest pressure measured by the Galileo probe as it descended into the atmosphere was 22 bar.

\*\* Highly tilted magnetic dipole.

Space Environment, Geochemistry, and Ranging (MESSENGER) mission (Anderson et al. 2007; Slavin et al. 2008) showed that the strength of Mercury's magnetic field was similar to that measured with *Mariner 10* in 1974. However, just like Earth's magnetosphere, it demonstrated short-term variability caused by the ever-changing solar wind (Fujimoto et al. 2008).

In contrast, Venus has a dense atmosphere and a very weak intrinsic magnetic field (Luhmann and Russell 1997). Its close proximity to the ionizing radiation of the Sun results in a large ionosphere. In this case, induced currents in the ionosphere generate local magnetic fields that stand off the plasma from the solar wind (Russell 1991).

Earth has a modest magnetic field and atmosphere. As the varying solar wind sweeps past, it can produce geomagnetic storms resulting, for example, in spectacular auroras around the magnetic poles. The Sun-Earth connection will be discussed in detail in Part IV of this series. The moon has basically no intrinsic magnetic field or atmosphere, so effectively casts a shadow or void in the solar wind on its leeward side.

Mars has a tenuous atmosphere and a patchy magnetic field. At the locations where the Martian magnetic field is at its strongest, it holds off the solar wind; however, where the field is weak, the solar wind can reach the surface. The Mars Atmosphere and Volatile Evolution (MAVEN) spacecraft revealed complex dynamics in the Martian magnetotail (DiBraccio et al. 2015).

The gas giants (Jupiter, Saturn, Uranus, and Neptune) interact differently with the solar wind. They have very strong magnetic fields and extensive, dense atmospheres. Thus, they have huge magnetospheres and ionospheres. Auroras have been observed on all of these gas giant planets. However, most of the magnetospheric dynamics are governed by internal processes rather than by the solar wind (Krupp 2014). Uranus and Neptune each have highly tilted dipolar fields that originate from conductive layers in the planetary atmosphere, rather than the planet's core, creating an even more complex interaction with the solar wind (Arridge 2015).

Comets interact with the solar wind in a spectacular way (see Fig. 5). As a comet is drawn into the inner solar system, solar radiation starts to evaporate gas and dust from the nucleus to form a tenuous cloud of particles around it: the coma. The comet leaves a trail of this material behind along its orbit, forming a bright curved tail that is often visible to the naked eye when illuminated by sunlight. If Earth's orbit should intersect with this trail, we see a meteor shower.



**FIG. 5. (bottom)** A comet has a bright tail caused by the scattering of sunlight off the dust and gases it leaves behind in its wake along its orbit. (top) The blue ion tail is created by the ionization of cometary gas from EUV radiation from the Sun, which then interacts with the charged particles and magnetic fields in the solar wind. (Source: image of Comet Hale Bopp in 1997 by E. Kolmhofer and H. Raab, Johannes Kepler Observatory, Linz, Austria.)

A second tail, the ion tail, formed by interaction of the comet with the solar wind, points directly away from the Sun. Induced currents flow through this newly ionized gas, creating a solar-wind-induced magnetosphere, complete with a magnetotail.

A class of comets, the so-called sun divers, rarely survive perihelion. They are reduced to clouds of dust and plasma high in the solar corona by the intense solar radiation, which are then swept away by the solar wind (e.g., Comet ISON or C/2012 S1). Only the largest sun-diver comets survive the encounter and then only if they can maintain their structural integrity (e.g., Comet Lovejoy or C/2011 W3).

As they approach the Sun, comets produce a range of different atmospheric conditions as more gas and dust is sublimed out from the nuclei forming ever denser comas. Thus, comets were actually the original solar wind probes, providing information on variations in the direction and speed of the solar wind at different distances from the Sun as they plunged into the inner solar system (Biermann 1951, 1957).

The variety of ambient conditions supplied by the different solar system objects is both a challenge and an opportunity for space weather physics to progress. Each provides a unique laboratory to test various aspects of our understanding of the solar wind interactions with a wide range of magnetic and atmospheric conditions.

## THE OUTER BOUNDARY OF THE SOLAR SYSTEM

**SYSTEM.** The Sun forms a teardrop-shaped magnetic cocoon in the interstellar medium (see Fig. 1), rather like that of Earth's magnetosphere in the solar wind. In the ram direction the outer boundary of the heliosphere is compressed, whereas in the opposite direction the heliosphere is stretched out into an elongated tail.

The interplanetary magnetic field becomes mostly azimuthal and perpendicular to the solar wind flow; here, solar transients and interplanetary shocks catch up with each other and form large global merged interaction regions typically beyond 2 au. In addition, more of the nominal solar wind is composed of photoionized interstellar neutral particles, known as pickup ions.

With increasing distance from the Sun, the particle and field pressure of the solar wind decreases as it starts to interact with interstellar matter. As the solar wind slows to less than its sound speed, it forms a shock wave called the termination shock. Eventually,

it reaches pressure balance with the local interstellar medium at a boundary called the heliopause; the transition region between these boundaries is called the inner heliosheath. The region beyond the heliopause, where the interstellar medium is affected by the presence of the heliosphere, is called the outer heliosheath. In the heliosheath the solar wind starts to deflect toward the heliotail and continues slowing.

Three different spacecraft are providing the first samples of this region. *Voyager 1* and *Voyager 2* are making in situ measurements of the solar wind farther out than has been achieved before. *Voyager 1*, launched in 1977, is currently over 137 au from the Sun. It crossed the termination shock in 2003 and the heliosheath in 2012. It is now believed to be sampling the interstellar medium. *Voyager 2*, launched a month before *Voyager 1*, crossed the termination shock in 2007, but because its trajectory was more in the ecliptic plane, it crossed this boundary about 10 au closer to the Sun than *Voyager 1*. As of 2017, it is 113 au from the Sun.

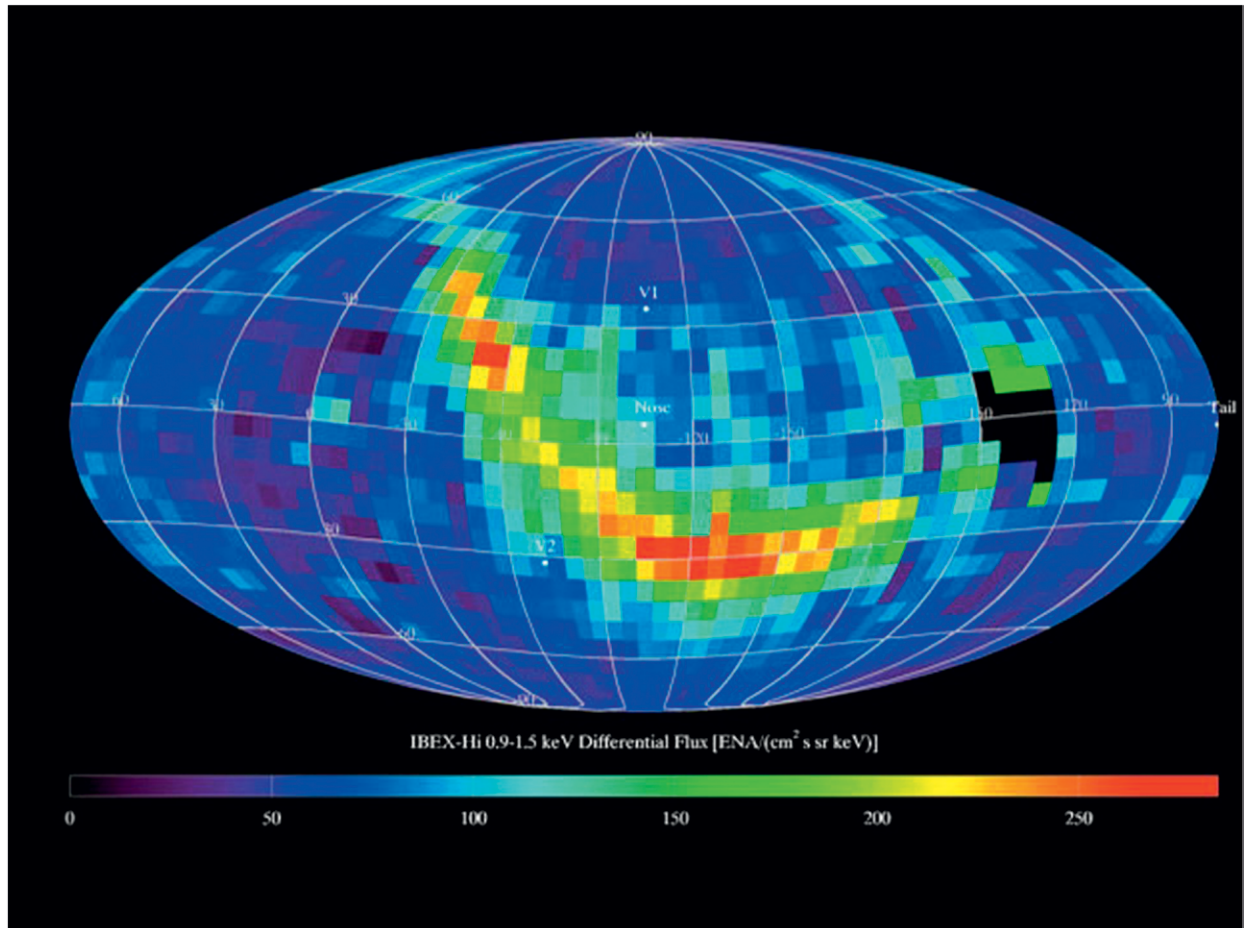


**FIG. 6. IBEX has made the first all-sky images of the outer boundary between the solar system and interstellar space. It not only revealed this unexpectedly bright ribbon of ENA emissions but also found that the structure of the ribbon is dynamic. (Source: NASA IBEX.)**

The Voyager missions take only in situ measurements, but a new observational technique, energetic neutral atom (ENA) imaging, is being used by the Interstellar Boundary Explorer (IBEX) mission (McComas et al. 2009) to remotely sense the entire heliopause (Fig. 6). The detectors measure the ENA fluxes from the outer heliosphere and perhaps local interstellar space. This allows IBEX to map the interactions between the solar wind and the interstellar gas at the outer boundary of our solar system. One discovery from IBEX is the presence of a bright, narrow ribbon at the outer boundaries of the solar system (Fig. 6) that surprisingly appears to vary (McComas et al. 2014).

The termination shock and heliosheath are thought by some to be the source of an extra, anomalous component of the cosmic rays observed on Earth (Potgieter 2013). Besides low-energy neutral particles, the extremely high-energy galactic cosmic rays can also enter the heliosphere, but not without first being modulated by the periodically varying heliospheric magnetic fields. Interactions between the heliosphere and galactic cosmic rays can become geoeffective. These charged particles are likely accelerated in supernovas and suffuse the galaxy with an anisotropic flux of high-energy electrons, protons, and heavy ions. The solar magnetic field diverts many of them away from the solar system. However, during solar minimum, as the large-scale solar magnetic field weakens and CMEs become less frequent, the flux of such particles in the inner solar system increases. They can affect living cells and microelectronics, which make them an issue for long-duration interplanetary manned flight.

**CONCLUSIONS.** The heliopause marks the limits that humans will be able to explore for the foreseeable future, perhaps forever. Thus, it is critical that we understand the nature and variability of the heliosphere if we are to travel regularly beyond the relatively safe cocoon of Earth's magnetosphere. That is where we turn next (in Part IV) to the local space environment around Earth known as geospace. Here, the various forms of energy released by the Sun and modulated in the heliosphere interact with Earth, its atmosphere, and its magnetic field to produce the space weather effects that could significantly impact our increasingly technology-dependent society.

**ACKNOWLEDGMENTS.** The authors thank the members of the Heliophysics Division at NASA GSFC for their help and support. The long-standing open-data policy of the heliophysics community has enabled all solar researchers to

investigate the effects of space weather in a more creative and cooperative way. NV is supported by a NASA Guest Investigator grant. This work was also supported by funding from the FedEx Institute of Technology at the University of Memphis.

## REFERENCES

- Anderson, B. J., M. H. Acuña, D. A. Lohr, J. Scheifele, A. Raval, H. Korth, and J. A. Slavin, 2007: The magnetometer instrument on MESSENGER. *Space Sci. Rev.*, **131**, 417–450, <https://doi.org/10.1007/s11214-007-9246-7>.
- Antiochos, S. K., Z. Mikic, V. S. Titov, R. Lionello, and J. A. Linker, 2011: A model for the sources of the slow solar wind. *Astrophys. J.*, **731**, 112–122, <https://doi.org/10.1088/0004-637X/731/2/112>.
- Arridge, C. S., 2015: Magnetotails of Uranus and Neptune. *Magnetotails in the Solar System*, A. Keiling, C. M. Jackman, and A. Delamere, Eds., John Wiley and Sons, 119–133, <https://doi.org/10.1002/9781118842324.ch7>.
- Biermann, L., 1951: Kometenschweife und solare Korpuskularstrahlung. *Z. Astrophys.*, **29**, 274–286.
- , 1957: Solar corpuscular radiation and the interplanetary gas. *Observatory*, **77**, 109–110.
- Cranmer, S. R., 2009: Coronal holes. *Living Rev. Sol. Phys.*, **6**, 3, <https://doi.org/10.12942/lrsp-2009-3>.
- De Pontieu, B., and Coauthors, 2014: The Interface Region Imaging Spectrograph (IRIS). *Sol. Phys.*, **289**, 2733–2779, <https://doi.org/10.1007/s11207-014-0485-y>.
- DiBraccio, G. A., and Coauthors, 2015: Magnetotail dynamics at Mars: Initial MAVEN observations. *Geophys. Res. Lett.*, **42**, 8828–8837, <https://doi.org/10.1002/2015GL065248>.
- Fisk, L. A., 2003: Acceleration of the solar wind as a result of the reconnection of open magnetic flux with coronal loops. *J. Geophys. Res.*, **108**, 1157–1164, <https://doi.org/10.1029/2002JA009284>.
- Fujimoto, M., W. Baumjohann, K. Kabin, R. Nakamura, J. A. Slavin, N. Terada, L. Zelenyi, 2008: Hermean magnetosphere-solar wind interaction. *Mercury, Space Sciences Series of ISSI*, Vol. 26, 347–368, [https://doi.org/10.1007/978-0-387-77539-5\\_12](https://doi.org/10.1007/978-0-387-77539-5_12).
- Geiss, J., and G. Gloeckler, 1998: Abundances of deuterium and helium-3 in the protosolar cloud. *Space Sci. Rev.*, **84**, 239–250, <https://doi.org/10.1023/A:1005039822524>.
- , —, and R. Von Steiger, 1995: Origin of the solar wind from composition data. *Space Sci. Rev.*, **72**, 49–60, <https://doi.org/10.1007/BF00768753>.
- Gilbert, H. R., K. T. Strong, and J. L. R. Saba, Eds., 2009: GSFC Heliophysics Science Division 2008 science highlights. NASA/TM-2009-214178, 185 pp.,

- <https://ntrs.nasa.gov/archive/nasa/casi.ntrs.nasa.gov/20090032603.pdf>.
- Harrison, R. A., and Coauthors, 1995: The Coronal Diagnostic Spectrometer for the Solar and Heliospheric Observatory. *Sol. Phys.*, **162**, 233–290, <https://doi.org/10.1007/BF00733431>.
- Howard, R. A., and Coauthors, 2008: Sun Earth Connection Coronal and Heliospheric Investigation (SECCHI). *Space Sci. Rev.*, **136**, 67–115, <https://doi.org/10.1007/s11214-008-9341-4>.
- Kasper, J. C., M. L. Stevens, A. J. Lazarus, J. T. Steinberg, and K. W. Ogilvie, 2007: Solar wind helium abundance as a function of speed and heliographic latitude: Variation through a solar cycle. *Astrophys. J.*, **660**, 901–910, <https://doi.org/10.1086/510842>.
- Krupp, N., 2014: Giant magnetospheres in our solar system: Jupiter and Saturn compared. *Astron. Astrophys. Rev.*, **22**, 75, <https://doi.org/10.1007/s00159-014-0075-x>.
- Luhmann, J., and C. T. Russell, 1997: Venus magnetic field and magnetosphere. *Encyclopedia of Planetary Sciences*, J. H. Shirley and R. W. Fainbridge, Eds., Chapman and Hall, 905–907.
- McComas, D. J., and Coauthors, 1998: Ulysses' return to the slow solar wind. *Geophys. Res. Lett.*, **25**, 1–4, <https://doi.org/10.1029/97GL03444>.
- , and Coauthors, 2007: Understanding coronal heating and solar wind acceleration: Case for in situ near-Sun measurements. *Rev. Geophys.*, **45**, RG1004, <https://doi.org/10.1029/2006RG000195>.
- , and Coauthors, 2009: IBEX—International Boundary Explorer. *Space Sci. Rev.*, **146**, 11–33, <https://doi.org/10.1007/s11214-009-9499-4>.
- , and Coauthors, 2014: IBEX: The first five years (2009–2013). *Astrophys. J.*, **213** (Suppl.), 20–47, <https://doi.org/10.1088/0067-0049/213/2/20>.
- Parker, E. N., 1958: Dynamics of the interplanetary gas and magnetic field. *Astrophys. J.*, **128**, 644–670.
- , 1989: Solar and stellar magnetic fields and atmospheric structures: Theory. *Solar and Stellar Flares*, B. M. Haisch and M. Rodonò, Eds., Springer, 271–288, [https://doi.org/10.1007/978-94-009-1017-1\\_18](https://doi.org/10.1007/978-94-009-1017-1_18).
- Potgieter, M. S., 2013: Solar modulation of cosmic rays. *Living Rev. Sol. Phys.*, **10**, 3, <https://doi.org/10.12942/lrsp-2013-3>.
- Pulkkinen, T., 2007: Space weather: Terrestrial perspective. *Living Rev. Sol. Phys.*, **4**, 1, <https://doi.org/10.12942/lrsp-2007-1>.
- Russell, C. T., Ed., 1991: *Venus Aeronomy*. Kluwer Academic, 489 pp., <https://doi.org/10.1007/978-94-011-3300-5>.
- Schwenn, R., 2006: Space weather: The solar perspective. *Living Rev. Sol. Phys.*, **3**, 2, <https://doi.org/10.12942/lrsp-2006-2>.
- Sheeley, N. R., 1999: Using LASCO observations to infer solar wind speed near the Sun. *AIP Conf. Proc.*, **471**, 41–45, <https://doi.org/10.1063/1.58784>.
- Slavin, J. A., and Coauthors, 2008: Mercury's magnetosphere after MESSENGER's first flyby. *Science*, **321**, 85–89, <https://doi.org/10.1126/science.1159040>.
- Strong, K. T., J. L. R. Saba, and T. A. Kucera, 2012: Understanding space weather: The Sun as a variable star. *Bull. Amer. Meteor. Soc.*, **93**, 1327–1335, <https://doi.org/10.1175/BAMS-D-11-00179.1>.
- , J. T. Schmelz, J. L. R. Saba, and T. A. Kucera, 2017: Understanding space weather. Part II: The violent Sun. *Bull. Amer. Meteor. Soc.*, **98**, 2387–2396, <https://doi.org/10.1175/BAMS-D-16-0191.1>.
- Viall, N. M., H. E. Spence, A. Vourlidas, and R. Howard, 2010: Examining periodic solar-wind density structures observed in the SECCHI heliospheric imagers. *Sol. Phys.*, **267**, 175, <https://doi.org/10.1007/s11207-010-9633-1>.
- Von Steiger, R., and Coauthors, 2000: Composition of quasi-stationary solar wind flows from Ulysses/Solar Wind Ion Composition Spectrometer. *J. Geophys. Res.*, **105**, 27 217–27 238, <https://doi.org/10.1029/1999JA000358>.
- Wang, Y. M., and N. R. Sheeley Jr., 1990: Solar wind speed and coronal flux tube expansion. *Astrophys. J.*, **355**, 726–732, <https://doi.org/10.1086/168805>.
- Wilcox, J. M., T. Hoeksema, and P. H. Scherrer, 1980: Origin of the warped current sheet. *Science*, **209**, 603–605, <https://doi.org/10.1126/science.209.4456.603>.